# Electronic Supplementary material to: Arctic Sea-ice Variations in the First Half of the 20th Century: A New Reconstruction Based on Hydrometeorological Data*

Vladimir A. SEMENOV[1,2], Tatiana A. ALDONINA[1,2], Fei LI[3], Noel Sebastian KEENLYSIDE[3,4], and Lin WANG[5]

[1]*A.M. Obukhov Institute of Atmospheric Physics RAS*, *Moscow* 119017, *Russia*

[2]*Institute of Geography RAS*, *Moscow* 119017, *Russia*

[3]*Geophysical Institute*, *University of Bergen and Bjerknes Centre for Climate Research*, *Bergen* 5007, *Norway*

[4]*Nansen Environmental and Remote Sensing Center*, *Bergen* 5007, *Norway*

[5]*Center for Monsoon System Research*, *Institute of Atmospheric Physics*, *Chinese Academy of Sciences*, *Beijing* 100029, *China*

**ESM to:** Semenov, V. A., T. A. Aldonina, F. Li, N. S. Keenlyside, and L. Wang, 2024: Arctic sea ice variations in the first half of the 20th century: A new reconstruction based on hydrometeorological data. *Adv. Atmos. Sci.*, **41**(8), 1483–1495, https://doi.org/10.1007/s00376-024-3320-x.

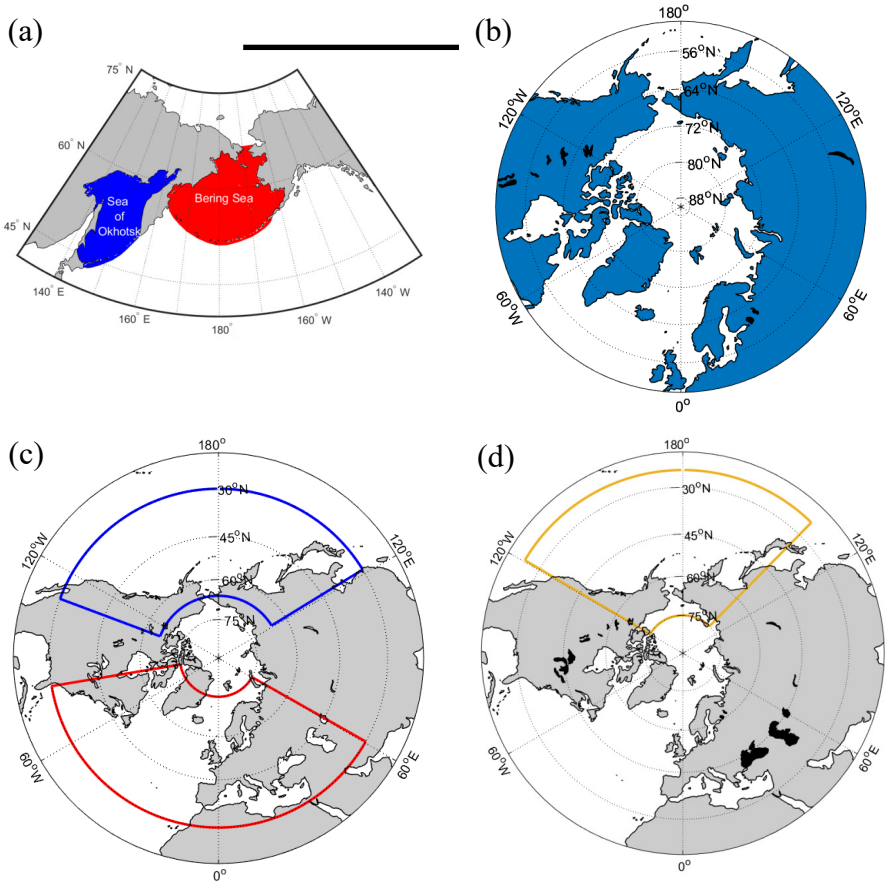


**Fig. S1.** (a) Regions of the Bering Sea and Sea of Okhotsk where SICs were calculated for two of the three regression models used in this study. Another model was built for the sea ice in the rest of the Northern Hemisphere (the Arctic Ocean including the Atlantic sector). (b) Land areas where EOFs of SAT anomalies were calculated. (c) Atlantic and Pacific regions where EOFs of SST anomalies were calculated. (d) Region where SLP EOFs were calculated. Latitudes/longitudes of the boxes and references to the data sources are in the text of the article.

*The online version of this article can be found at https://doi.org/10.1007/s00376-024-3320-x.

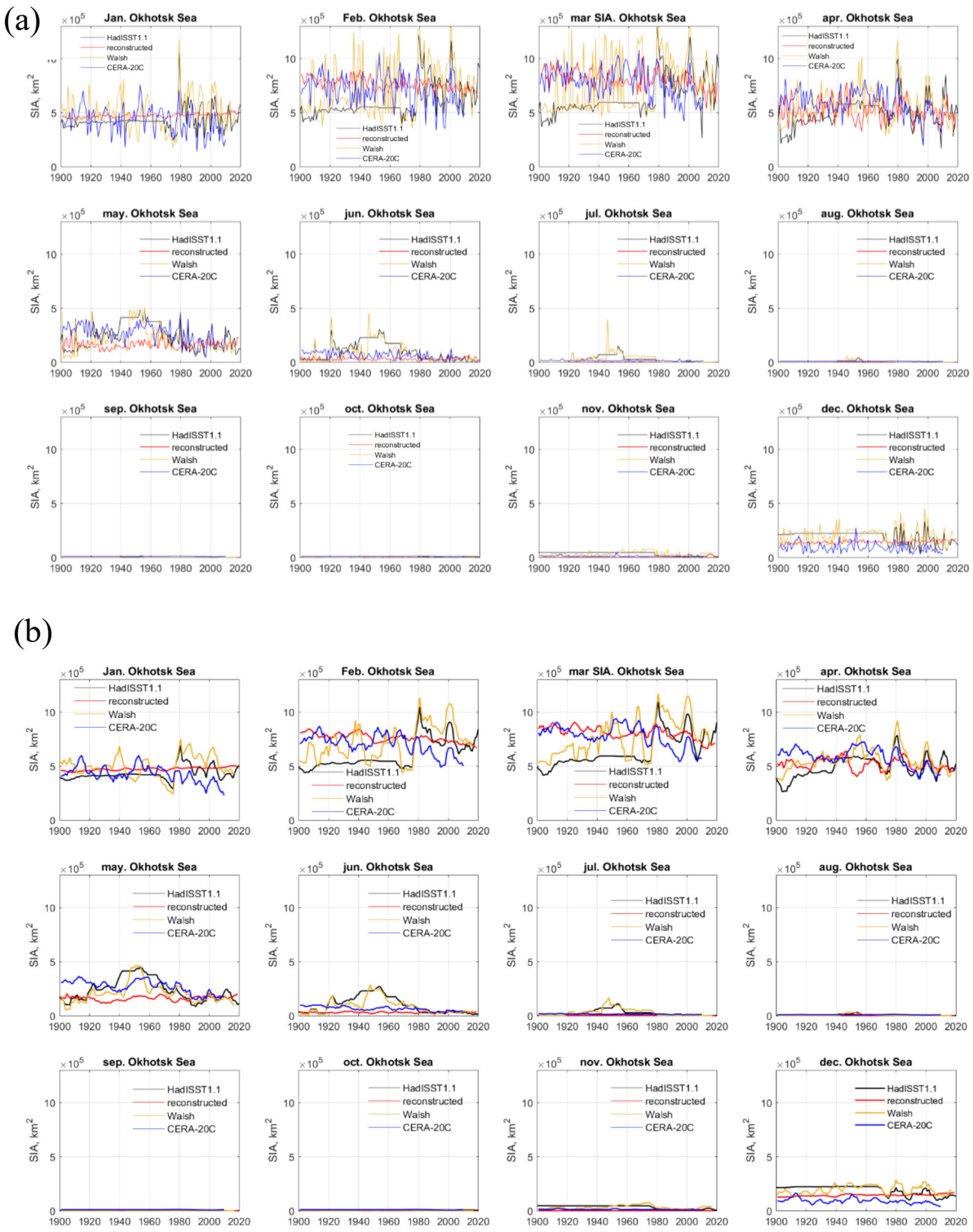


**Fig. S2.** SIA (units: km$^2$) in the Sea of Okhotsk for different months according to HadISST1.1 (black), SIBT1850 (yellow), the reconstructed data (red), and the CERA20C (blue) coupled reanalysis (Laloyaux et al., 2016), with (a) annual resolution and (b) 5-year running mean smoothing.

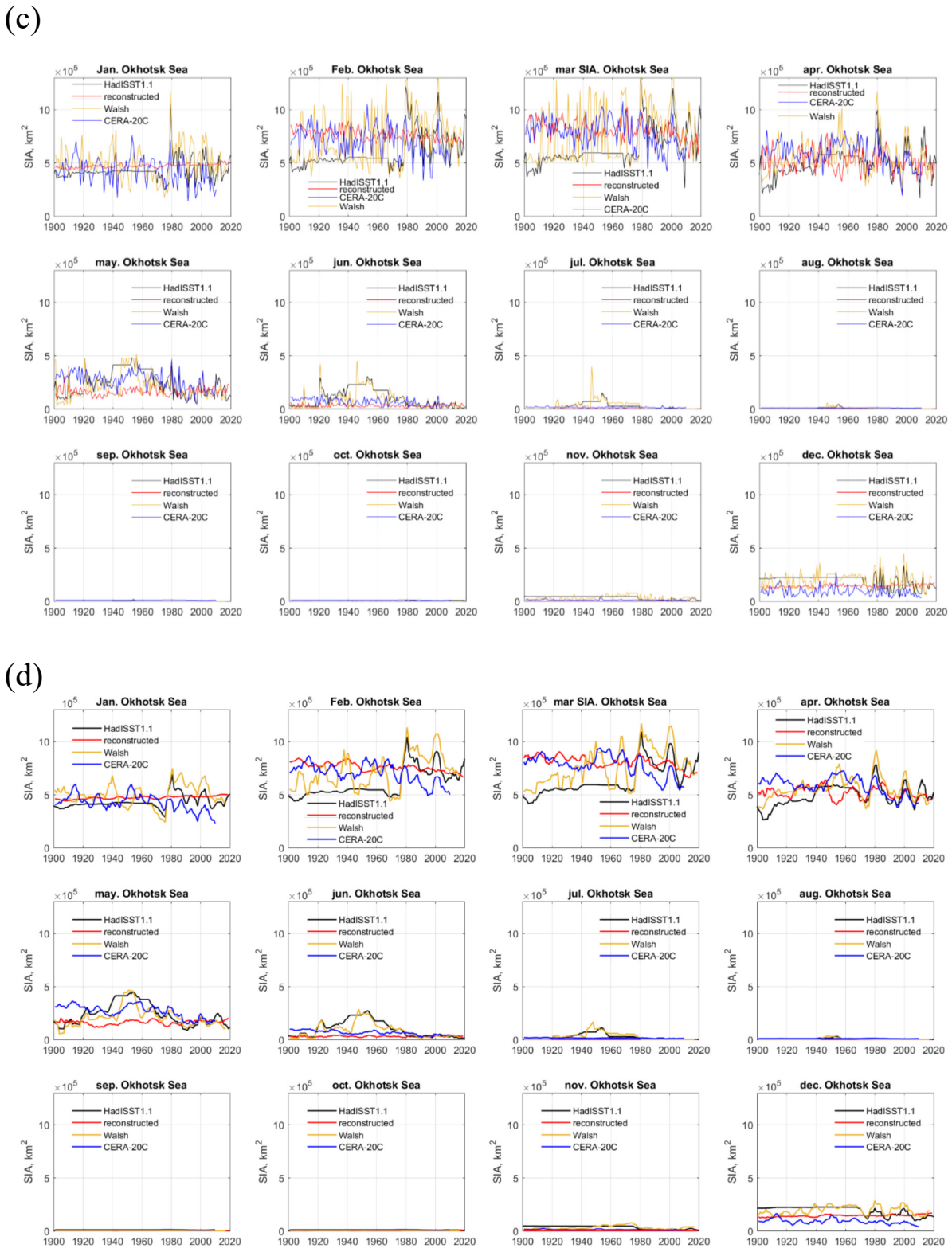


**Fig. S2.** (continued). SIA (units: km$^2$) in the Sea of Okhotsk for different months according to HadISST1.1 (black), SIBT1850 (yellow), the reconstructed data (red), and the ERA20C (blue) atmosphere reanalysis (Poli et al., 2016), with (c) annual resolution and (d) 5-year running mean smoothing.

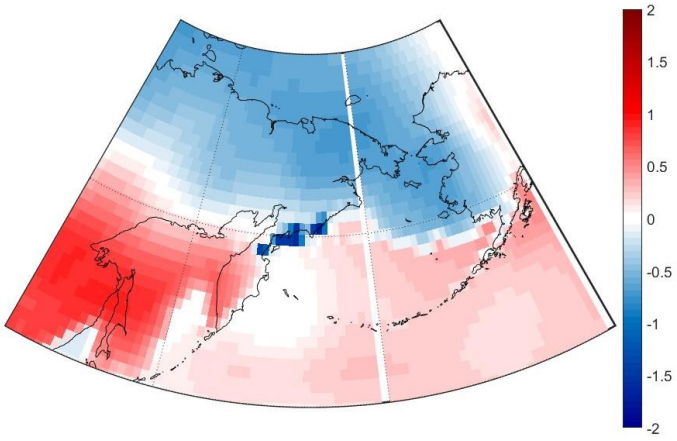


**Fig. S3.** March SST/SAT trends for the period 1915–45 [K (10 yr)$^{-1}$] according to the GISSTEMP v4 temperature analysis (Lenssen et al., 2019).

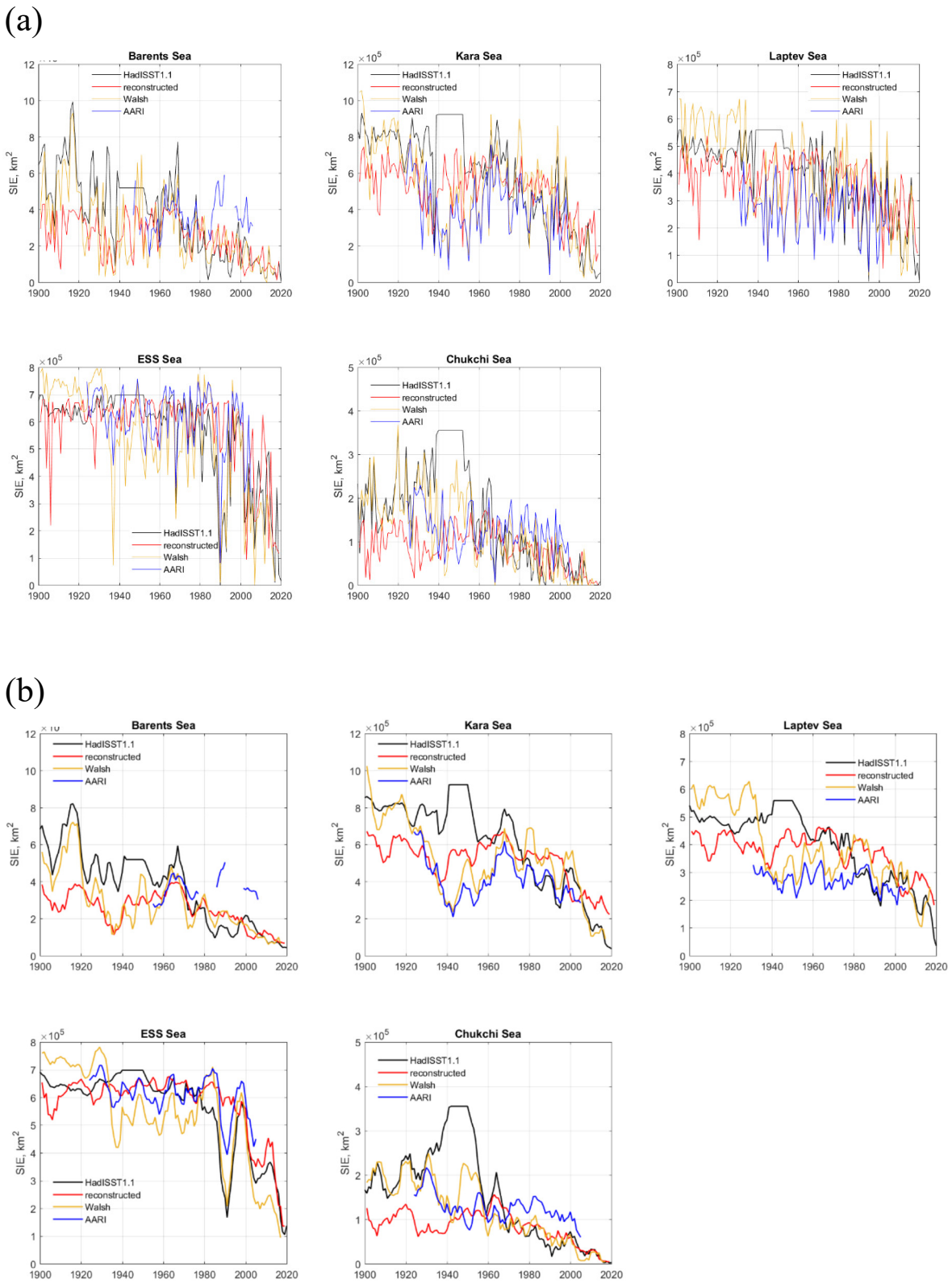


**Fig. S4.** August SIE (units: km$^2$) in the different seas of the Eastern Arctic according to HadISST1.1 (black), SIBT1850 (yellow), the reconstructed data (red), and Polyakov et al. (2003) data (blue), with (a) annual resolution and (b) 5-year running mean smoothing.

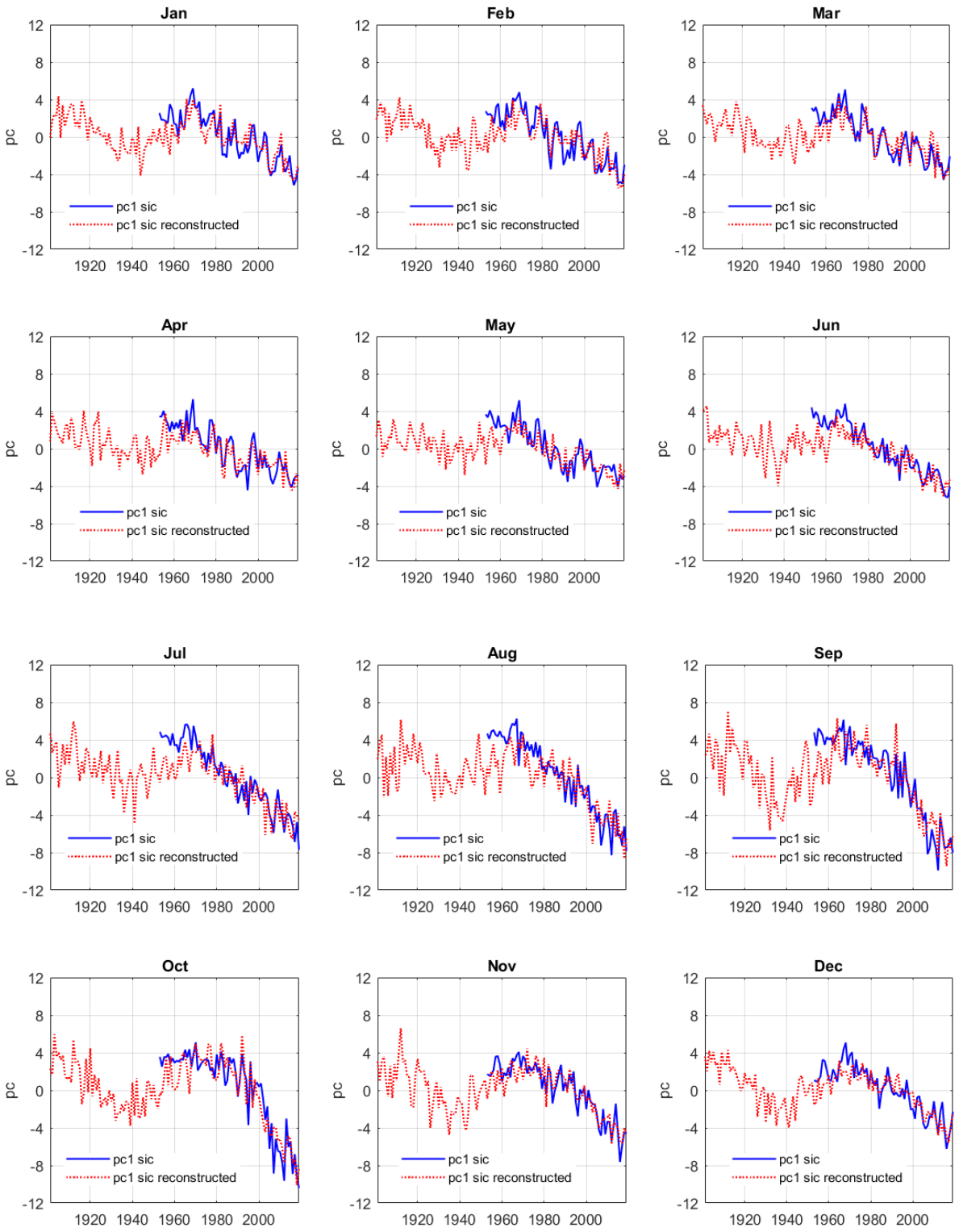


**Fig. S5.** PC of the first EOF of SIC from HadISST1.1 (blue) and as reconstructed (red) for all months.

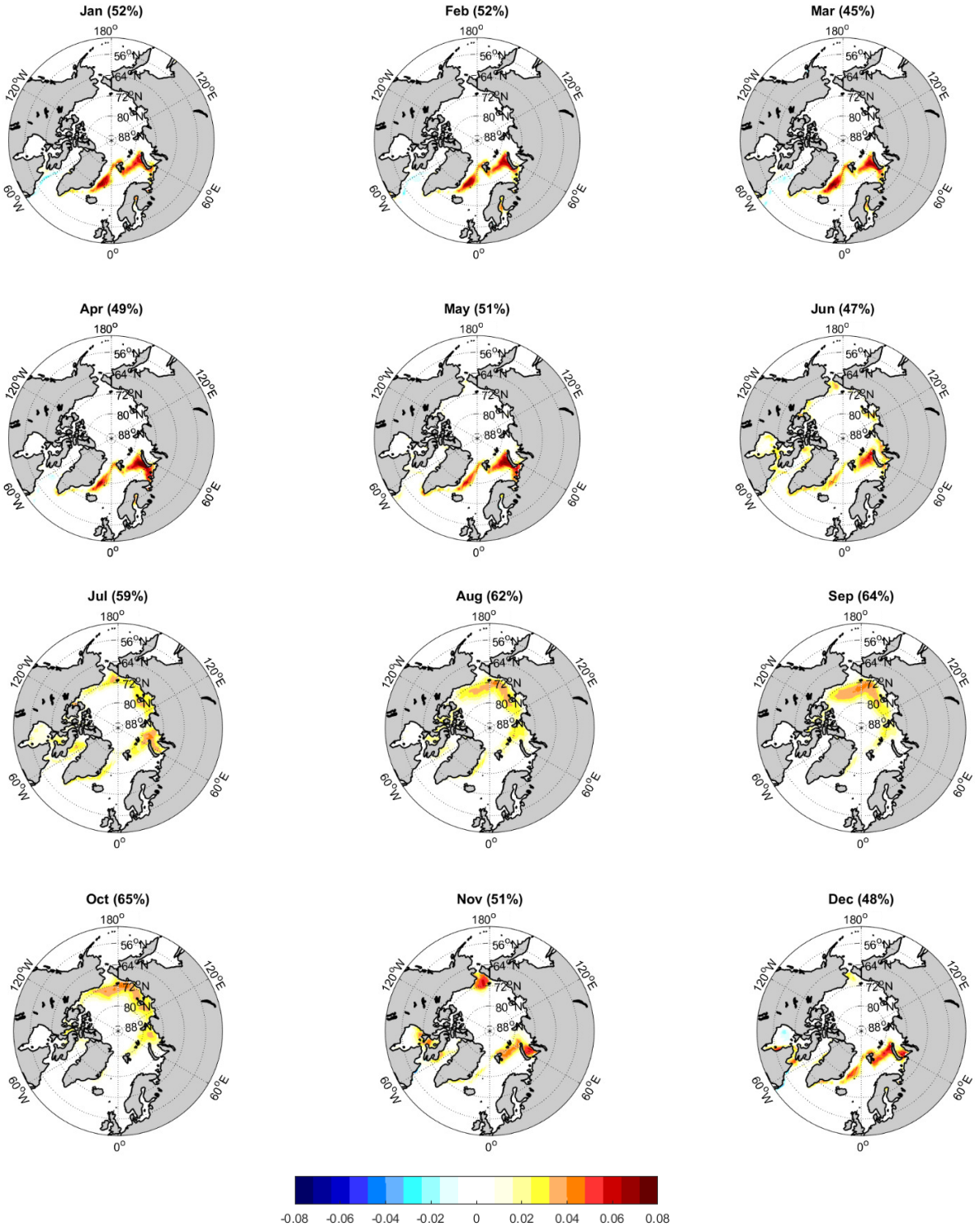


**Fig. S6.** First EOF of SIC from the HadISST1.1 dataset for the period 1953–2019 for all months. Explained variability is shown in parentheses.

**Table S1**. Variability of March and September SIC PCs (in %) explained by different predictor PCs in the regression model for the Arctic (except the Bering Sea and the Sea of Okhotsk) during the 1953–2019 training period. NA, North Atlantic; NP, North Pacific (see Fig. S1).

March

| Predictor\SIC | SIC PC1 | SIC PC2 | SIC PC3 | SIC PC4 | SIC PC5 | SIC PC6 |
|---|---|---|---|---|---|---|
| SAT PC1 | 9 | 2 | 3 | 31 | 0 | 14 |
| SAT PC2 | 0 | 3 | 0 | 15 | 1 | 1 |
| SAT PC3 | 2 | 2 | 2 | 2 | 5 | 7 |
| SAT PC4 | 0 | 1 | 6 | 1 | 1 | 3 |
| SST NA PC1 | 58 | 5 | 8 | 4 | 6 | 6 |
| SST NA PC2 | 1 | 51 | 37 | 12 | 62 | 2 |
| SST NA PC3 | 3 | 7 | 0 | 0 | 8 | 2 |
| SST NA PC4 | 0 | 1 | 14 | 0 | 0 | 35 |
| SST NP PC1 | 0 | 16 | 13 | 2 | 5 | 1 |
| SST NP PC2 | 10 | 1 | 13 | 23 | 0 | 4 |
| SST NP PC3 | 3 | 7 | 5 | 2 | 7 | 25 |
| SST NP PC4 | 15 | 5 | 1 | 7 | 5 | 0 |

September

| Predictor\SIC | SIC PC1 | SIC PC2 | SIC PC3 | SIC PC4 | SIC PC5 | SIC PC6 |
|---|---|---|---|---|---|---|
| SAT PC1 | 12 | 1 | 1 | 46 | 11 | 8 |
| SAT PC2 | 2 | 2 | 16 | 5 | 6 | 16 |
| SAT PC3 | 1 | 2 | 4 | 0 | 13 | 4 |
| SAT PC4 | 5 | 8 | 0 | 7 | 4 | 2 |
| SST NA PC1 | 58 | 6 | 0 | 20 | 2 | 1 |
| SST NA PC2 | 1 | 15 | 0 | 2 | 3 | 1 |
| SST NA PC3 | 3 | 16 | 6 | 10 | 6 | 4 |
| SST NA PC4 | 3 | 9 | 47 | 1 | 5 | 3 |
| SST NP PC1 | 2 | 10 | 0 | 0 | 5 | 35 |
| SST NP PC2 | 7 | 4 | 15 | 4 | 12 | 1 |
| SST NP PC3 | 4 | 3 | 9 | 1 | 18 | 0 |
| SST NP PC4 | 0 | 24 | 1 | 4 | 15 | 25 |

## Supplementary figures and tables

## REFERENCES


Laloyaux, P., M. Balmaseda, D. Dee, K. Mogensen, and P. Janssen, 2016: A coupled data assimilation system for climate reanalysis. *Quart. J. Roy. Meteor. Soc.*, **142**, 65–78, https://doi.org/10.1002/qj.2629.

Lenssen, N. J. L., G. A. Schmidt, J. E. Hansen, M. J. Menne, A. Persin, R. Ruedy, and D. Zyss, 2019: Improvements in the GISTEMP uncertainty model. *J. Geophys. Res.: Atmos.*, **124**(12), 6307–6326, https://doi.org/10.1029/2018JD029522.

Poli, P., and Coauthors, 2016: ERA-20C: An atmospheric reanalysis of the twentieth century. *J. Climate*, **29**, 4083–4097, https://doi.org/10.1175/JCLI-D-15-0556.1.

Polyakov, I. V., and Coauthors, 2003: Long-term ice variability in Arctic marginal seas. *J. Climate*, **16**, 2078–2085, https://doi.org/10.1175/1520-0442(2003)016<2078:LIVIAM>2.0.CO;2.